Designing the Fourier space with transformation optics

Jensen Li,[1] Seunghoon Han,[1] Shuang Zhang,[1] Guy Bartal,[1] and Xiang Zhang[1,2,*]

[1]*NSF Nanoscale Science and Engineering Center (NSEC), 3112 Etcheverry Hall, University of California, Berkeley, California 94720-1740, USA*

[2]*Materials Science Division, Lawrence Berkeley National Laboratory, 1 Cyclotron Road, Berkeley, California 94720, USA*

**Corresponding author: xiang@berkeley.edu*

Received May 18, 2009; revised August 19, 2009; accepted September 9, 2009; posted September 16, 2009 (Doc. ID 111585); published October 7, 2009

We show that transformation optics can be applied to extend the functionalities of conventional optical devices. In particular, geometrically compressing the input facet of any conventional optical elements can extend the input spatial frequency bandwidth. As an example, we design a Fourier lens that can transform the image to its reciprocal space and operate for incident light of subwavelength profile. An explicit design employing metal–dielectric layers is given for realization. © 2009 Optical Society of America

OCIS codes: 230.3205, 070.7345, 160.3918.

Transformation optics (TO) with metamaterials permits the manipulation of the light flow at will by artificially reshaping the electromagnetic space, through the spatially inhomogeneous permittivity and permeability distribution [1,2]. It has led to the most compelling demonstration of an invisibility cloak at microwave frequencies [3]. Indeed, the implications of TO go beyond cloaking and provide a new paradigm in designing optical components. Recently, TO has been applied to reshaping free space to achieve various additional optical components, such as a field concentrator, rotator, and beam splitter [4–6], and to transport a real space image, such as the impedance-matched hyperlens, flat hyperlens, and complementary media [7–14].

In this Letter, we develop a generic approach combining TO with conventional optics to transform an electromagnetic space to provide a broader bandwidth in the spatial frequency domain. As an example, we design a Fourier lens to transform the real to the reciprocal space of the image, so that a subwavelength profile can be resolved. This complementary control in both real and reciprocal space is especially emphasized in Fourier optics for applications such as a spatial frequency filter for optical information processing.

An optical Fourier transform can be obtained by a Fraunhofer diffraction, converging lens, or graded-index (GRIN) medium [15,16]. However, all of them work only within the paraxial regime [15]. They have a small input bandwidth, so that the Fourier transform can be accurate only up to a fraction of the wavenumber of the background medium. Utilizing TO, we can increase the spatial frequency bandwidth of the device. While TO is usually applied in transforming homogeneous media, here the untransformed space is a GRIN medium [17] with the following refractive index profile:

$$n(x') = n_1(1 - \pi^2 x'^2/8f^2), \tag{1}$$

where f is the focal length and $n(x')$ (with maximum n_1) is truncated for values less than 1. Figure 1(a) shows the schematic with TM polarization (2D) assumed for simplicity. At $z'=f$, the Fourier transformed signal is

$$H(x'',f) \propto \int H(x',0)\exp(-i\kappa x')\mathrm{d}x', \tag{2}$$

where $H(x',0)$ and $H(x'',f)$ are the input and the output signal for the H field in the y direction. A position x'' at $z'=f$ represents the spatial frequency κ by [16]

$$\kappa = n_1 k_0 \pi x''/2f, \tag{3}$$

where k_0 is the wavenumber of vacuum.

Next, we apply TO on the device through a coordinate map [Fig. 1(b)]. The input facet is compressed by a factor of N ($N>1$) while the output facet remains the same size, D. As any input signal being compressed in the real space is expanded by the same

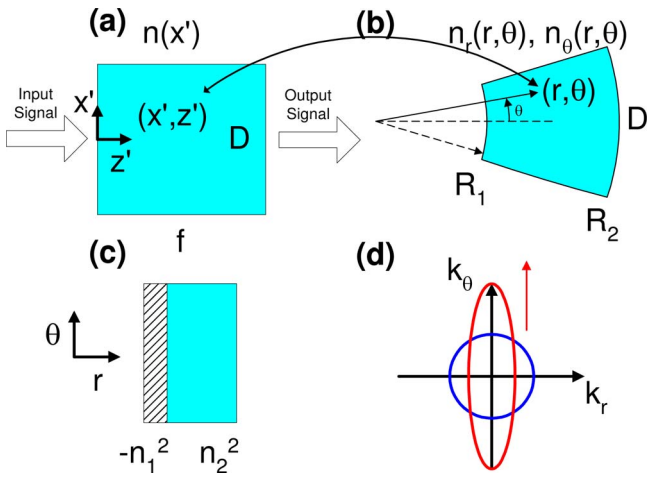

Fig. 1. (Color online) (a) The rectangular GRIN medium is geometrically compressed at the input and is transformed into (b) a cylindrical shell. (c) Metamaterial building block for the system shown in (b). (d) Expansion (shown by the red arrow) of the paraxial regime shown in reciprocal space from circular (blue circle, the original dielectric) to elliptical (red ellipse, the metal–dielectric-based metamaterial).

amount in its spatial frequency spectrum, an N-times enhancement for the input bandwidth is generic for any optical device. In particular, we choose a map from a rectangle to a cylindrical shell, given by

$$x' = R_2\theta,$$

$$z' = (r^2 - R_1^2)/2R_2, \tag{4}$$

where (x', z') and (r, θ) are the Cartesian and cylindrical coordinates before and after the map from Figs. 1(a) and 1(b). R_1 and R_2 are the inner and outer radii of the lens. The input interface is compressed by a factor of $N = R_2/R_1$, which is also the bandwidth enhancement. The input field at $r = R_1$ is Fourier transformed at $r = R_2$. By coordinate transformation [Eq. (4)], the GRIN medium [Eq. (1)] is transformed to a new anisotropic medium with radial and azimuthal indices of refraction:

$$n_r(r, \theta) = \frac{r}{R_2} n_1 \left(1 - \frac{\pi^2 R_2^2 \theta^2}{8f^2}\right),$$

$$n_\theta(r, \theta) = \frac{R_2}{r} n_1 \left(1 - \frac{\pi^2 R_2^2 \theta^2}{8f^2}\right), \tag{5}$$

where $f = (R_2^2 - R_1^2)/2R_2$. The position $R_2\theta$ at the outer interface represents the spatial frequency κ of the input signal at R_1 as

$$\kappa = \frac{R_2}{R_1} \frac{n_1 k_0 \pi}{2f} R_2\theta. \tag{6}$$

While Eq. (5) describes the effective medium profile for the cylindrical Fourier lens, we choose to provide a feasible implementation of this medium by using metamaterials, with a unit building block shown in Fig. 1(c). It is constructed from metal layers of permittivity $-n_1^2$ and dielectric GRIN layers of refractive index $n_2 = n_1(1 - \delta)$ stacking alternately along the r direction. η is the filling ratio of the metal, and δ represents the graded dielectric profile as a function of (r, θ). The thicknesses of the layers are subwavelength ($< \lambda/5$ in design). The effective indices in the direction perpendicular and parallel to the layers (up to the first order of δ) can be obtained by using effective medium theory [18],

$$n_r = n_1 \left(1 - \frac{1 - \eta}{1 - 2\eta}\delta\right)(1 - 2\eta)^{1/2},$$

$$n_\theta = n_1 \left(1 - \frac{1 - \eta}{1 - 2\eta}\delta\right)(1 - 2\eta)^{-1/2}. \tag{7}$$

Therefore, by varying η and δ, we can control the shape and the size of the equifrequency contour gradually over the element. The original device has a bandwidth limited by the highest available dielectrics. By introducing anisotropy through the metal layers (without dielectrics of index higher than n_1), n_θ is increased with a decrease in n_r. This elongated equifrequency contour [Fig. 1(d)] expands the paraxial regime ($k_\theta << n_\theta k_0$), where the elliptical dispersion can be approximated by using a parabola $k_r \approx n_r(k_0 - k_\theta^2/(2k_0 n_\theta^2))$, thereby expanding the Fourier transform operation of the lens to a larger bandwidth and reaching subwavelength resolution when n_θ is large enough.

The detailed design for the metamaterial Fourier lens can be obtained by equating Eqs. (5) and (7). The filling ratio of the metal layers (a function of r) is given by

$$\eta(r) = 1/2 - r^2/2R_2^2, \tag{8}$$

and the dielectric GRIN layers between the metal layers have the refractive index profile

$$n_2(r, \theta) = n_1 \left(1 - \frac{2R_2^2}{R_2^2 + r^2} \frac{\pi^2 r^2 \theta^2}{8f^2}\right). \tag{9}$$

We set $R_1 = 14.4$ μm, $R_2 = 21.6$ μm, and $n_1 = 1.5$ for the metamaterial Fourier lens immersed in a glass background of refractive index 1.5. Figure 2 shows the whole structure. The metal layers are Ag (with permittivity $-2.25 + 0.26i$ at the working wavelength of 360 nm [19]), and the GRIN layers can be obtained by drilling subwavelength grooves or holes in glass [17]. The filling ratio η decreases from 0.278 at the inner to 0 at the outer radius to improve impedance matching ($dz'/dr = 1$ at $r = R_2$). The period of each bilayer is 72 nm. Only the first 66 Ag layers (from the inner radius) thicker than 8 nm are constructed, while the remaining ones are dropped for simplification, which does not affect the performance of the device. The index profile of the GRIN medium is implemented according to Eq. (9) with truncation to 1 (the air) for values less than 1.

To verify the optical Fourier transform action of the metamaterials lens, we performed full-wave simulation using the COMSOL Multiphysics solver [Fig. 3(a)]. A cylindrical wave is impinging on an absorp-

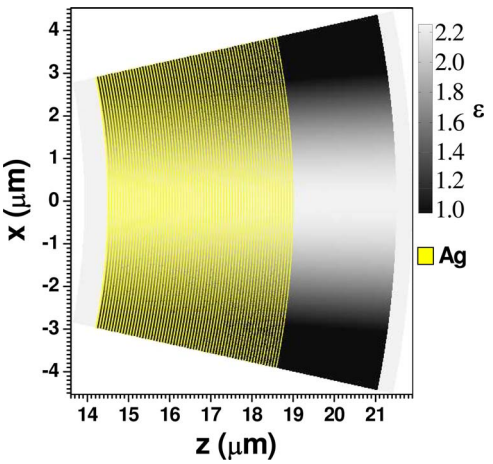

Fig. 2. (Color online) Detail of implementation using metal–dielectric multilayers to construct the Fourier lens with an effective medium [Eq. (5)]. The 66 yellow (light gray) concentric layers are Ag ($\varepsilon = -2.25 + 0.26$, while the gray-scale map is the permittivity profile of the GRIN medium (maximum index of 1.5 for white) interlacing with them.

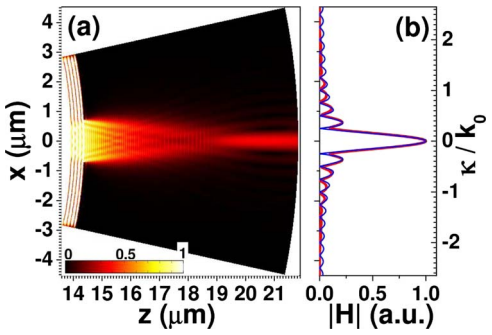

Fig. 3. (Color online) (a) Optical Fourier transform (plotted amplitude) of a rectangular input function from the device at a wavelength of 360 nm. (b) The amplitude of the Fourier transform at the lens output is shown in red (thicker gray), while the blue curve (thinner black) corresponds to the ideal one.

tive screen (made of Cr) with aperture width $a = 1.44\ \mu$m in front of the lens at R_1. The rectangle aperture function (width a) is optically Fourier transformed at R_2 with the H field amplitude plotted in Fig. 3(b) in red (dark gray) while the ideal Fourier transformed signal (amplitude of sinc function, normalized against the fundamental peak for comparison) is shown in blue (lighter gray). A good match between them is obtained up to $R_2\theta \approx 2.2\ \mu$m. That is, higher input spatial frequency components ranging to $\kappa \sim 1.3k_0$ [Eq. (6), with subwavelength features] are optically Fourier transformed at the curved output Fourier plane (R_2).

Finally, we evaluate the amplitude transfer function [15] of the metamaterial Fourier lens (from input at R_1 to output at R_2) by considering a Dirac δ function as the input signal. The δ input function is approached by narrowing a Gaussian function at the input of the lens until the spatial frequency spectrum obtained at the lens output does not change with further narrowing. When its amplitude is compared with the corresponding result for the original GRIN lens before applying TO (Fig. 4), the input bandwidth (the largest κ before the exponential drop of the transfer amplitude) is apparently increased by around 40% for the transformed lens. It is very close

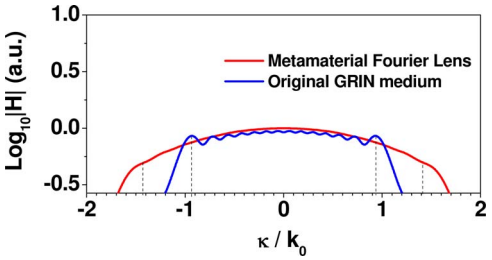

Fig. 4. (Color online) Magnitude of the amplitude transfer function at output interface R_2 for the transformed lens (red smooth curve) and the GRIN medium before transformation (blue wavy curve). A flat response is expected for an ideal Fourier lens. Only data points that fall within the lens diameter are shown.

to the expectation value $R_2/R_1 = 1.5$, despite several approximations (effective medium of the metal–dielectric layers, material loss in Ag, and truncation of the index profile) adopted in implementation. A further increase in the input bandwidth can be achieved by increasing the ratio between the outer and the inner radius of the device.

In conclusion, we have demonstrated the use of TO in designing a Fourier lens that can resolve subwavelength features. A detailed implementation using metal–dielectric layers is given and supported by simulations. We have shown that the bandwidth in spatial frequency for the device can be increased by 40% with respect to a conventional GRIN lens and hence extends to the subwavelength regime. Our approach also provides a generic way to combine conventional and transformation optics.

We acknowledge financial support from the U.S. Army Research Office (ARO) MURI program 50432-PH-MUR and the National Science Foundation Nano-scale Science and Engineering Center (NSF-NSEC) under award CMMI-0751621.

References

1. J. B. Pendry, D. Schurig, and D. R. Smith, Science **312**, 1780 (2006).
2. U. Leonhardt, Science **312**, 1777 (2006).
3. D. Schurig, J. J. Mock, B. J. Justice, S. A. Cummer, J. B. Pendry A. F. Starr, and D. R. Smith, Science **314**, 977 (2006).
4. M. Rahm, S. A. Cummer, D. Schurig, J. B. Pendry, and D. R. Smith, Phys. Rev. Lett. **100**, 063903 (2008).
5. H. Chen, B. Hou, S. Chen, X. Ao, W. Wen, and C. T. Chan, Phys. Rev. Lett. **102**, 183903 (2009).
6. A. Greenleaf, Y. Kurylev, M. Lassas, and G. Uhlmann, Phys. Rev. Lett. **99**, 183901 (2007).
7. A. V. Kildishev and E. E. Narimanov, Opt. Lett. **32**, 3432 (2007).
8. Z. Liu, H. Lee, Y. Xiong, C. Sun, and X. Zhang, Science **315**, 1686 (2007).
9. Y. Xiong, Z. Liu, and X. Zhang, Appl. Phys. Lett. **94**, 203108 (2009).
10. A. V. Kildishev and V. M. Shalaev, Opt. Lett. **33**, 43 (2008).
11. S. Han, Y. Xiong, D. Genov, Z. Liu, G. Bartal, and X. Zhang, Nano Lett. **8**, 4243 (2008).
12. X. Zhang and Z. Liu, Nat. Mater. **7**, 435 (2008).
13. S. Anantha Ramakrishna, J. B. Pendry, M. C. K. Wiltshire, and W. J. Stewart, J. Mod. Opt. **50**, 1419 (2003).
14. J. B. Pendry and S. Anantha Ramakrishna, J. Phys. Condens. Matter **15**, 6345 (2003).
15. J. W. Goodman, *Introduction to Fourier Optics* (McGraw-Hill, 1996).
16. D. Mendlovic and H. M. Ozaktas, J. Opt. Soc. Am. A **10**, 1875 (1993).
17. U. Levy, M. Abashin, K. Ikeda, A. Krishnamoorthy, J. Cunningham, and Y. Fainman, Phys. Rev. Lett. **98**, 243901 (2007).
18. D. Bergmann, Phys. Rep. **43**, 377 (1978).
19. J. B. Johnson and R. W. Christy, Phys. Rev. B **6**, 4370 (1972).